

A REVIEW OF AERONAUTICAL FATIGUE INVESTIGATIONS IN ISRAEL

APRIL 2005 – MARCH 2007

**Compiled by:
Abraham Brot
Engineering Division
Israel Aerospace Industries
Ben-Gurion Airport, Israel**

abrot@iai.co.il

SUMMARY

This review summarizes fatigue and fracture-mechanics investigations that were performed in Israel during the period April 2005 to March 2007. The review includes contributions from Israel Aerospace Industries Ltd. (IAI), Israel Air Force (IAF), Technion – Israel Institute of Technology, Tel-Aviv University, Ben-Gurion University and The Hebrew University of Jerusalem.

**Presented at the 30th ICAF Conference
Naples, Italy
15 May 2007**

TABLE OF CONTENTS

	Page
11.1 INTRODUCTION	11/3
11.2 FATIGUE ANALYSIS, TESTING AND LIFE EXTENSION	11/3
11.2.1 An Evaluation of the Strip-Yield Retardation Model for Crack Growth Prediction under Spectrum Loading (A. Brot and C. Matias, IAI)	11/3
11.2.2 Determining Crack Growth and Arrest Capability of Integrally Machined Structures by Analysis and Testing (A. Brot and Y. Peleg-Wolfin, IAI)	11/4
11.2.3 An Evaluation of Various Methods for Producing Initial Flaws for Fatigue Testing (C. Matias, IAI)	11/6
11.2.4 Autofrettaged Thick-Walled Cylinders (M. Perl et al, Ben-Gurion University)	11/7
11.2.5 Residual Tensile Stresses Induced by a Cold-Working a Fastener Hole (A. Brot and C. Matias, IAI)	11/7
11.2.6 G150 Executive Jet Fatigue Substantiation Program (A. Hermelin and S. Afnaim, IAI)	11/10
11.2.6.1 G150 Full-Scale Fatigue Test (A. Hermelin and S. Afnaim, IAI)	11/10
11.3 STRUCTURAL INTEGRITY AND HEALTH MONITORING OF COMPOSITE MATERIALS	11/11
11.3.1 Comprehensive Structural Integrity of Composites (Z. Granot, IAI and S. Gali, Consultant)	11/11
11.3.2 Smart Bonded Composite Patch Repairs – Analysis and Testing (I. Kressel, IAI, S. Gali, Consultant, et al)	11/12
11.3.3 Damage Detection in Composite Materials (P. Pevzner, A. Berkovits et al, Technion)	11/13
11.3.4 Structural Health Monitoring for Composite Structures Based on Lamb Wave Detection (P. Botsev et al, Tel Aviv University; I. Kressel et al, IAI and S. Gali, Consultant)	11/14
11.4 PROBABILISTIC STUDIES	11/15
11.4.1 Evaluating Probability of Second Layer Detection by Using Low-Frequency Eddy-Current NDI (C. Matias, A. Brot and W. Senderowits, IAI)	11/15
11.4.2 Fatigue Life Estimation Reliability (Y. Rabinowicz and Y. Roman, Hebrew University of Jerusalem)	11/17
11.5 MISCELLANEOUS	11/17
11.5.1 Stress Intensity Functions in the Neighborhood of Edges in a Three-Dimensional Linear Elastic Body (Z. Yosibash, N. Omer, et al, Ben-Gurion University)	11/17
11.5.2 Linear Elastostatic Problems in the Vicinity of Reentrant Corners (Z. Yosibash, E. Priel et al, Ben-Gurion University)	11/18
11.5.3 Cracks in Anisotropic Materials and Delamination in Fiber Reinforced Composites (L. Banks-Sills, Tel-Aviv University)	11/19
11.5.4 Crack Detection, Without Remeshing, Using a Genetic Algorithm (D. Rabinovic and D. Givoli, Technion)	11/20
11.5.5 Health Monitoring of Structural Joints (B. Karp, D. Rittel and D. Durban, Technion)	11/23
11.5.6 Fleet Usage Spectrum Evaluation and Mission Classification (M. Ben-Noon, IAF)	11/24
11.5.7 Lessons Learned from Historical Aircraft Accidents (A. Brot, IAI)	11/26
11.6 REFERENCES	11/27

A REVIEW OF AERONAUTICAL FATIGUE INVESTIGATIONS IN ISRAEL APRIL 2005 – MARCH 2007

11.1 INTRODUCTION

The Israel National Review summarizes work performed in the field of aeronautical fatigue in Israel during the period April 2005 to March 2007. The previous National Review [1] covered aeronautical fatigue activities up to March 2005. The following organizations contributed to this review:

Israel Aerospace Industries Ltd. (IAI)
Israel Air Force (IAF)
Technion – Israel Institute of Technology
Tel-Aviv University
Ben-Gurion University
Hebrew University of Jerusalem

The National Review was compiled by Abraham Brot of IAI (abrot@iai.co.il).

11.2 FATIGUE ANALYSIS, TESTING AND LIFE EXTENSION

11.2.1 An Evaluation of the Strip-Yield Retardation Model for Crack Growth Prediction under Spectrum Loading (A. Brot and C. Matias, IAI)

It is well established that, under spectrum loading, load-interaction effects occur which generally retard the rate of crack growth. This effect can be very significant — for certain types of loading spectra, the life increase due to retardation may be a factor ranging from 1.5 to 5.

Unfortunately, it is very difficult to predict a priori the extent of retardation that can be expected for a specific combination of alloy, loading spectrum, stress level and crack configuration.

Several load-interaction models have been proposed in the past 30 years, including the Wheeler, Willenborg, Generalized Willenborg, Closure and GRF Models. It has been found that these semi-empirical models have limited value in predicting crack growth behavior, since their dominating parameters must be “calibrated” for the specific alloy, loading spectrum, stress level and crack configuration. Since this calibration process can be performed only after crack growth testing, these methods are not very useful in predicting, during the design process, the expected crack growth life.

The present study includes 7475-T7351 and 7050-T7451 aluminum alloy coupons, which have been tested under a gust and maneuver spectrum, corresponding to a transport aircraft wing. The test coupons include two crack configurations: “center-cracked tension” (CCT) and “open hole” (OH). The test results were evaluated using the NASA developed “Strip-Yield Model” contained in NASGRO (version 5) software. It has previously been shown that this type of spectrum (high R-ratio) presents a severe challenge to currently used load-interaction models.

The study examined several ways to represent the cycle-by-cycle loading spectrum for crack growth interaction analysis. The spectrum can be simply randomized into discrete flights, as is shown in Figure 1 for a selected flight profile (flight number 58) taken from the 2000 flight block used for testing. The spectrum can be manipulated so that the peak load in each flight is paired directly with the minimum loading of that flight, as is shown in Figure 2. Alternately, this pairing process can be performed using “rainflow” or “range-pair” cycle-counting. All these techniques were evaluated relative to the measured test results. The use of an “empirical da/dN correction constant” was also be used in order to improve the correlation between the calculated crack growth curve and the measured data. In all cases, the emphasis was on using the Strip-Yield Retardation model with a minimal need for calibration.

Typical results, comparing the crack growth analysis to the measured test results, are shown in Figure 3. The results show that the Strip-Yield Retardation Model has undergone a significant improvement from version 4.22 to version 5.01 of NASGRO, for predicting crack growth behavior for a transport aircraft wing spectrum. On the other hand, it still does not correlate sufficiently well with the test data, especially for the CCT coupons, and an

empirical da/dN correction constant, applied to the Strip-Yield results, is still needed to improve the correlation to the test results.

The results of the study will be presented at the ICAF 2007 Symposium [2].

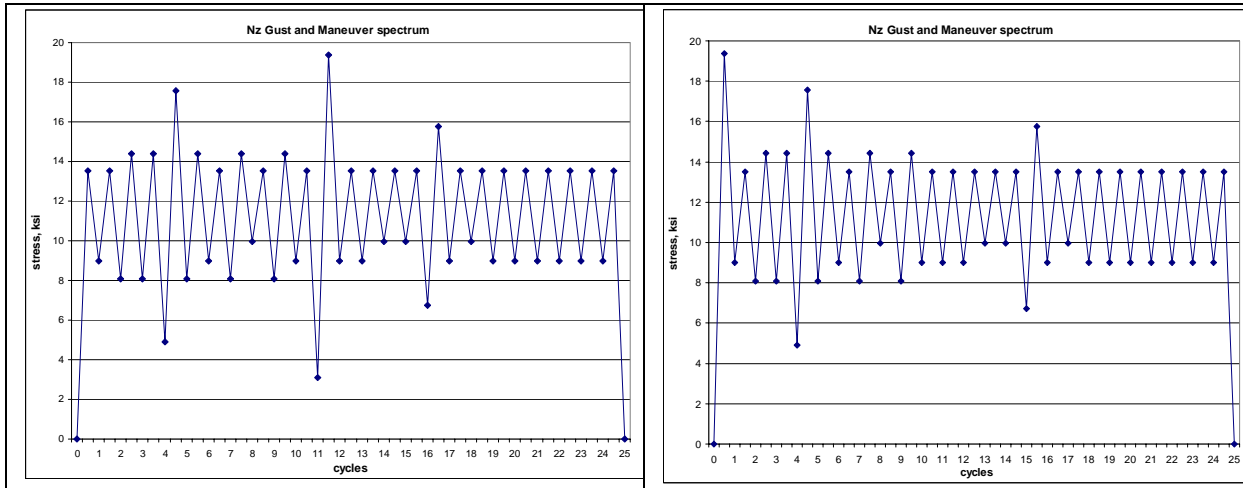


Figure 1: A Selected Test Flight Profile

Figure 2: Peak Load Paired with Minimum Load

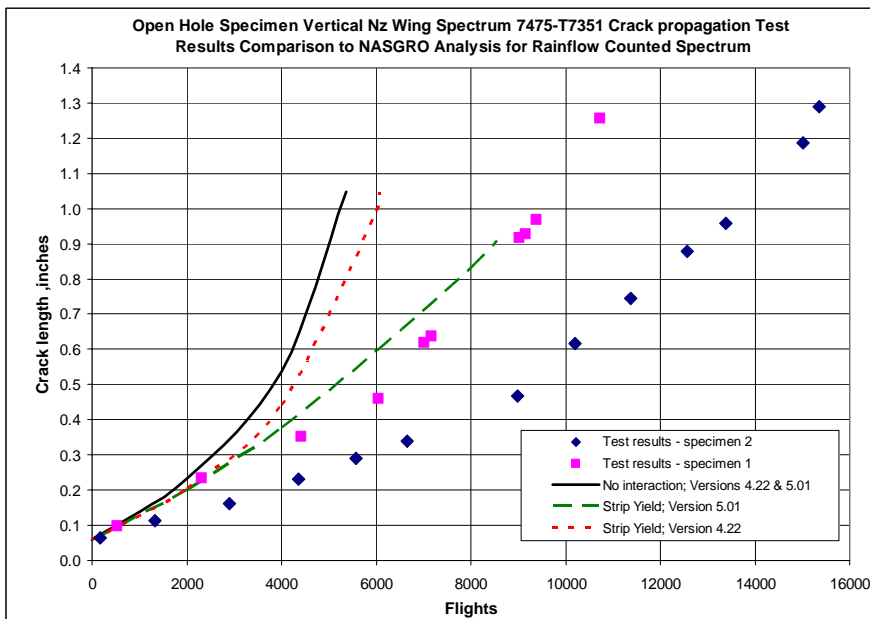


Figure 3: Calculated Crack Growth Results Compared to Test Data for NASGRO versions 4.22 and 5.01 (7475-T7351 alloy, Open-Hole Coupons)

11.2.2 Determining Crack Growth and Arrest Capability of Integrally Machined Structures (A. Brot and Y. Peleg-Wolfin, IAI)

IAI is a member of an international consortium in a project called **DaToN** (*Innovative Fatigue and Damage Tolerance Methods for the Application of New Structural Concepts*), which is *partially* funded by the European Commission. This project is aimed at developing new damage tolerance assessment tools that will deal with specific problems introduced by the use of integral structures manufactured by high-speed cutting, laser-beam welding or friction stir welding.

In the framework of the DaToN project, IAI performed a crack growth analysis of a seven integral stiffener panel, with the center stiffener broken and a $\pm 15\text{mm}$ skin crack. A p-version finite-element model was built, using StressCheck software. Stress-intensities were calculated by performing J-integral calculations with

StressCheck. When the skin crack reached a stiffener, various combinations of cracks in the stiffener and skin were considered, and the stress-intensities were calculated for all the combinations, as is shown in Figure 4. The resulting stress-intensities were input into NASGRO ver. 5 as a two-dimensional table (skin cracks and stiffener cracks), and the crack growth history was calculated accordingly. Figure 5 shows the calculated results obtained compared to the test data. Although the calculated results do not correspond precisely with the test results, the method of calculating the stress-intensities in the skin and stiffener showed very good correlation to the cracking sequence between the skin and stiffener.

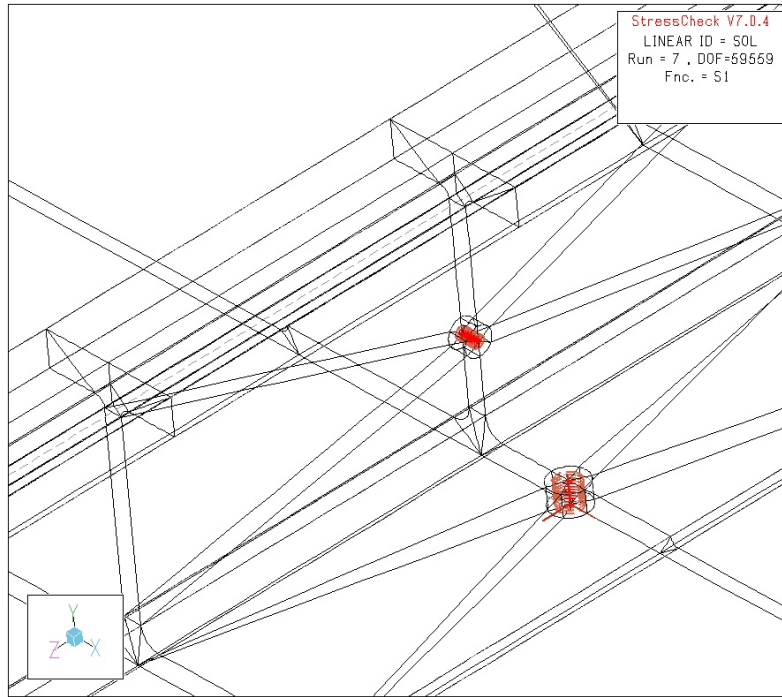


Figure 4: Calculation of Stress-Intensities (J-Integral) using a p-version FEM (StressCheck)

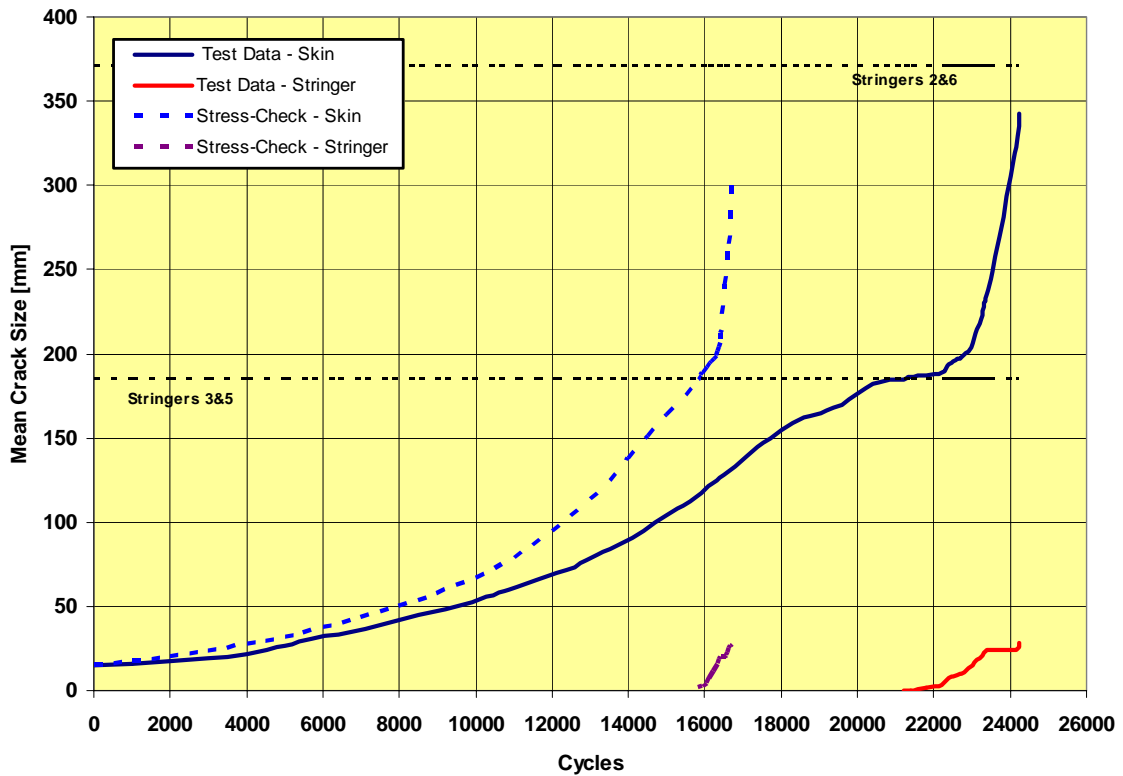


Figure 5: Calculated Crack Growth Curve Compared to Test Results

A test program is being carried-out on 2024-T351 panels containing two integral stiffeners, with the aim of determining the crack growth and residual strength characteristics. Figure 6 shows a failed panel in the testing machine.

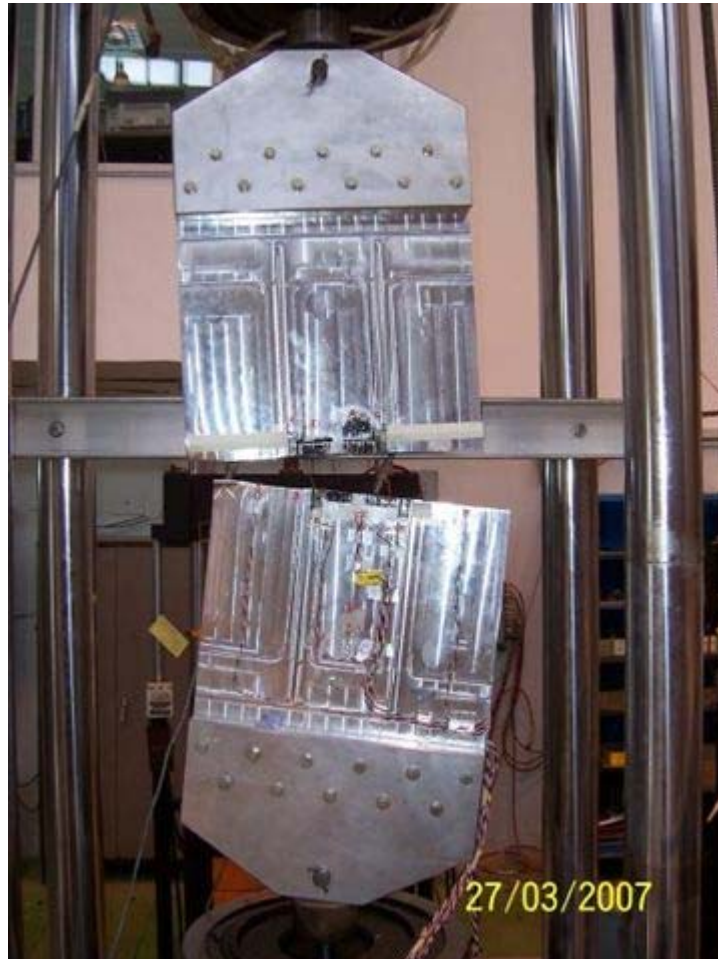


Figure 6: Integral Stiffener Panel Failure under Cyclic Loading Test

11.2.3 An Evaluation of Various Methods for Producing Initial Flaws for Fatigue Testing (C. Matias, IAI)

Initial flaws are often inflicted on a test-specimen in order to evaluate crack growth characteristics. Sometimes, a long delay occurs until a crack develops from the flaw. Testing was performed using open-hole specimens which were loaded to 15 ksi ($R = 0.05$). Figure 7 shows test results for the number of cycles required to initiate a crack, for various sized initial flaws that have been produced by two methods (EDM versus an 8/0 blade jeweler's saw).

The following conclusions are derived from the results:

- EDM produced initial flaws result in shorter delays than the 8/0 jeweler's saw.
- A crack growth delay of 0 – 13,000 cycles was found for flaws inflicted by the 8/0 jeweler's saw.
- Through-the-thickness initial flaws result in shorter delays in initiating cracks than part-through flaws.
- Part-through flaws should be at least 0.15" x 0.15" in order to result in a minimal delay.

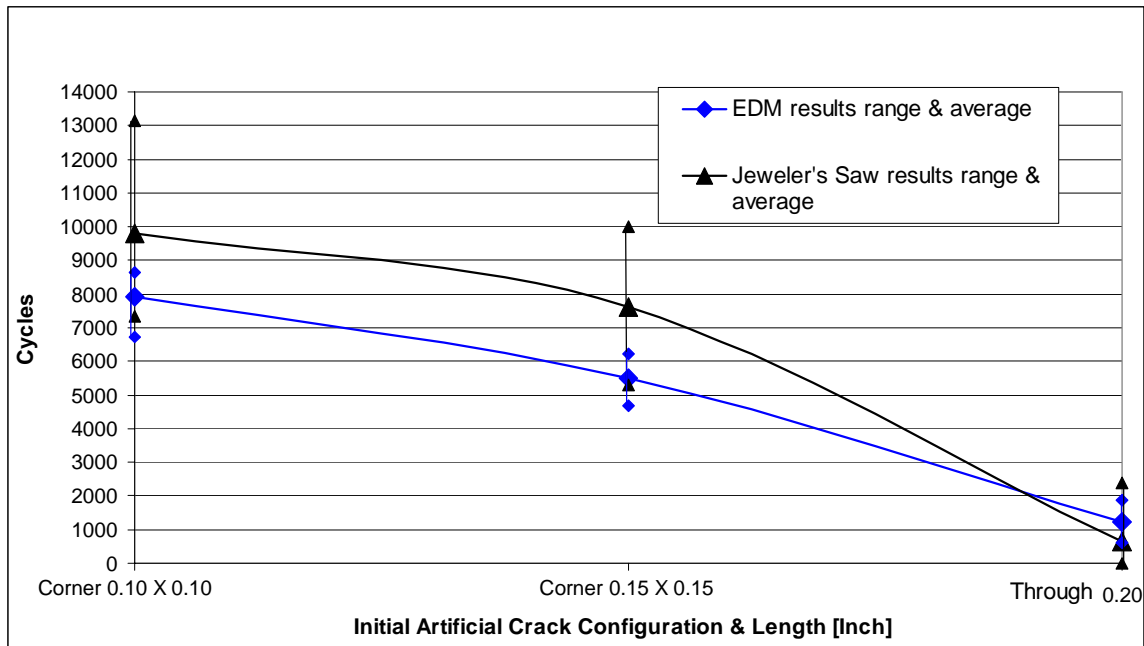


Figure 7: Crack growth Delay for Two Initial Flaw Methods

11.2.4 Autofrettaged Thick-Walled Cylinders (M. Perl et al, Ben-Gurion University)

Autofrettage of large diameter tubes (gun barrels) is used to increase the elastic strength of the tube and to increase its fatigue life. It is based on the permanent expansion of the cylinder bore using either hydraulic pressure or an oversize mandrel. The theoretical solution of the autofrettage problem involves different yield criteria, the Bauschinger effect and the recalculation of the residual stress field after machining. Accurate stress-strain data is needed for the numerical analysis of the residual stress field due to autofrettage. Although this topic does not relate directly to aeronautical fatigue, it was included in this review because of the similarity of the autofrettage process to that of the cold-working process that is used extensively in aircraft structures.

A study was performed to develop a 3D numerical solution which includes the Bauschinger effect. This model is capable of determining the stresses, strains, displacements and forces throughout the autofrettage process. The numerical results were validated by experimental measurements. The model gave excellent correlation to the measured mandrel forces and the permanent enlargement of the bore. The calculated tangential and axial stresses were not sufficiently consistent with the measurements, and are under further investigation [3].

Another study dealt with the influence of the Bauschinger effect on the combined (mode I) stress-intensity factor of an autofrettaged thick-walled cylinder. The Bauschinger effect was originally defined as the phenomenon whereby plastic deformation causes a loss of yield strength restraining in the opposite direction. A 3D finite-element analysis was performed employing sub-modeling technique and singular elements along the crack front. More than 1200 different crack configurations were analyzed. The Bauschinger effect was found to have a dramatic detrimental impact on the fatigue life of the cylinder [4 - 6].

11.2.5 Residual Tensile Stresses Induced by a Cold-Working a Fastener Hole (A. Brot and C. Matias, IAI)

During a spectrum component fatigue test, a crack initiated at a notched edge near a cold-worked fastener hole and propagated towards the hole, as is shown in Figure 8. Strain-gages, mounted at the 10mm notch, indicated a peak spectrum stress of about 50 - 60 ksi (notch stress). Fractographic analysis confirmed that the crack initiated at the edge and grew towards the hole. Since the maximum measured stress in the notch was not sufficiently high to explain crack-initiation during the test, it was suspected that the tensile residual stresses at the edge contributed to the cracking.

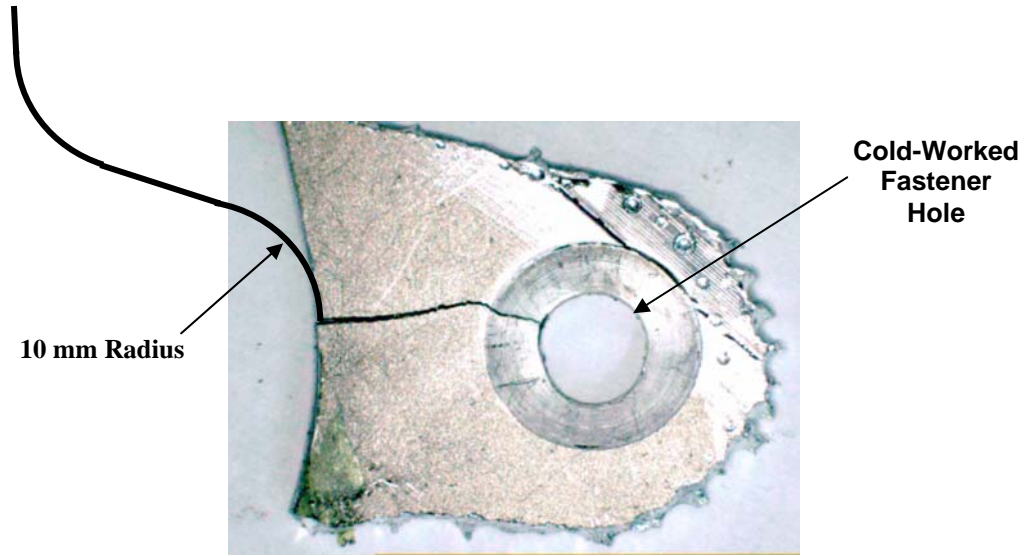


Figure 8: Crack Growth from a Notched Edge towards a Cold-Worked Fastener Hole (detail was cut-away from a component test specimen)

An experimental study was initiated in order to measure the tensile residual stresses induced by cold working. All the specimens were manufactured from 7475-T7351 aluminum alloy and the fastener holes were reamed and countersunk after cold-working. The specimens were produced in three configurations, having a 10mm notch, a 30mm notch and a straight edge. Stresses at the edges were measured after cold-working and then after final reaming and countersinking of the fastener holes. Residual stresses up to 35 ksi were measured. Figure 9 shows the measured residual stress distribution along the 10mm radius, while Figure 10 shows the measured residual stresses as a function of hole edge distance (e/D).

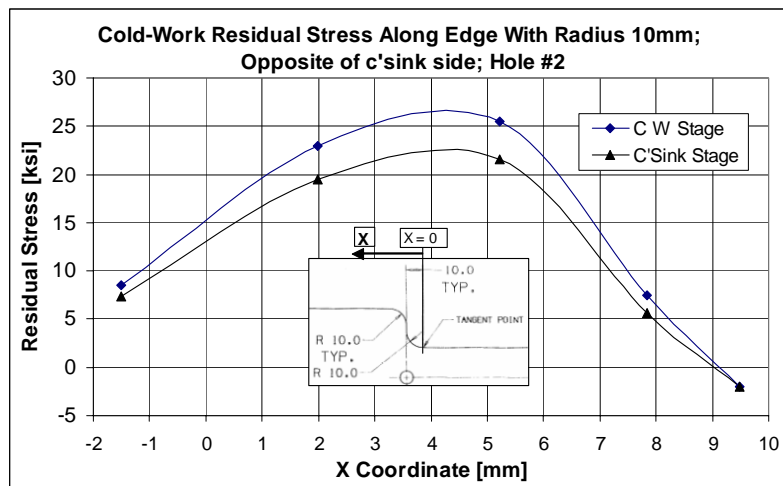


Figure 9: Stress Distributions along Edge of 10mm Notch Radius (opposite countersink)

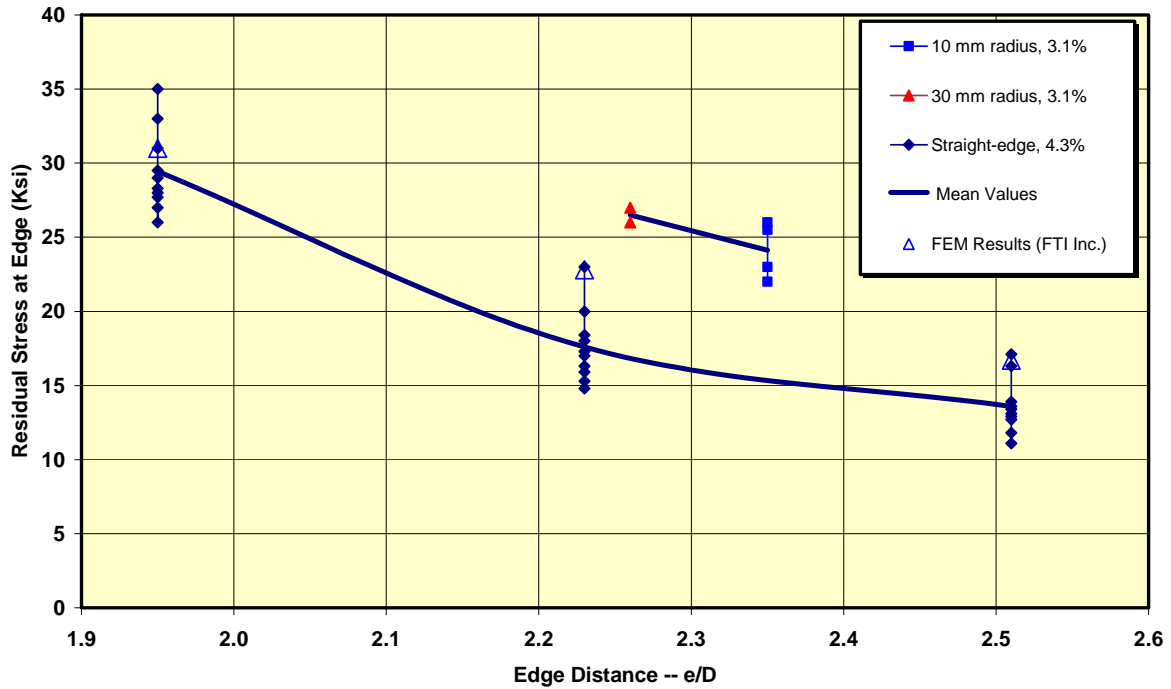


Figure 10: Measured Residual Stresses at Edge Resulting From Cold-Working

Finite-element analysis (FEA) was performed, using ABAQUS software to build the elastic-plastic model. This FEA was performed in order to validate the experimental results of cold-working near a straight edge. The results showed reasonably good agreement with the experimental results, especially for $e/d = 1.95$, where a maximum compressive stress of about -58 ksi at the bore of the hole and a maximum tensile stress of about 31 ksi at the edge was found.

A parametric fatigue analysis was performed in order to evaluate the effect of tensile residual stresses at a notch. Constant-amplitude loading with maximum *notch* stresses of 30, 40 and 50 ksi were taken, superimposed with residual stresses of 0, 10, 20 and 30 ksi. The effect that the residual stress has on the mean fatigue life was determined. For example, for a 40 ksi maximum *notch* stress, a 10 ksi tensile residual strength will reduce the mean fatigue life by a factor of 3.4.

For designing aircraft structures, sufficient distance between a cold-worked hole and an edge should be used, in order to minimize the residual tensile stresses. When the nearby edge contains a notch, the situation is especially critical.

From these results, it was concluded:

1. Testing and analysis confirm that high tensile residual stresses exist at an edge near a cold-worked hole.
2. These induced residual stresses are a function of: the edge-distance to hole diameter ratio, the level of mandrel interference, the existence (and characteristics) of a notch near the cold-worked hole, whether the fastener hole was final reamed and countersunk and the fit of the fastener that was installed...
3. When these residual stresses are combined with high cyclic notch stresses that arise from external loading, the fatigue life at the edge can be drastically reduced. This should be accounted for in the design details near a cold-worked hole.
4. Additional analysis and testing is needed to further quantify these effects.

These results were presented at the 47th Israel Annual Conference on Aerospace Sciences [7].

11.2.6 G150 Executive Jet Fatigue Substantiation Program (A. Hermelin and S. Afnaim, IAI)

Israel Aerospace Industries and Gulfstream Aerospace Corporation have completed the development of the G150, midsize executive jet. The G150 has transcontinental (USA) range and a maximum cruise speed of Mach 0.85. It can transport up to eight passengers in an executive configuration. The G150 is powered by two TFE 731 jet engines. The G150 primary structure is metallic except for the ailerons, elevators and landing gear doors that are manufactured from composite materials.

The G150 was certified by the CAA of Israel and the FAA in December 2005.

11.2.6.1 G150 Full-Scale Fatigue Test (A. Hermelin and S. Afnaim, IAI)

As part of the damage-tolerance certification, a G150 test-article has been tested for two lifetimes (40,000 flights) of fatigue and is being tested for approximately another half-lifetime (10,000 flights) of damage-tolerance testing.

The test-article included the fuselage and both wings. The tested areas consisted of the forward fuselage and cabin to the aft pressure bulkhead and fuel tank. Both entire wings were fatigue tested. Since the aft fuselage and empennage have not changed significantly from the G100 model, they were not fatigue tested and acted only as load application elements. The test aircraft was mounted to the test fixture at the nose landing gear attachment and at the engine mount fittings, as is shown in Figure 11. Figure 12 contain several photographs of the full-scale fatigue test.



Figure 11: Schematic Representation of the G150 Full-Scale Fatigue Test Setup



Figure 12: G150 Executive Jet Full-Scale Fatigue Test (Center Photo: After Completing 40,000 Flights)

The fatigue spectrum loading consists of randomly selected flight-by-flight sequences, reflecting the anticipated usage of the aircraft. A flight consists of the various flight and ground events that the aircraft will experience. 24 events per flight are included in the 2000 flight spectrum block.

The test-article has been divided into 20 loading zones, each of which is independently loaded during each event of the spectrum, using 30 servo-hydraulic actuators. In addition, the passenger cabin is pressurized, using compressed-air during the airborne events of the spectrum. The zone loading for each event has been determined using a “constrained least-square error method” which minimized deviations in loading of the important structural parameters. More than 1000 strain-gages have been bonded on the test-article, before and during the test, to monitor the onset of cracking and obtain stress level in areas where cracking has occurred.

The test has already accomplished the first part of the test program: two lifetimes of fatigue testing (40,000 flights) were completed in December 2006 with a total elapsed time of 15 months.

No major failures were observed during the entire fatigue test. A total of 18 cracks were detected as follows:

<u>Location</u>	<u>Number of Cracks Detected</u>
Aft Pressure Bulkhead	5
Wings	11
Wing Carry-Through Structure	1
Cockpit	1

Some of the cracks were repaired, and the effectiveness of the repair scheme was checked on the test-article, or on a production aircraft, by strain measurements. At some locations, where cracking would not endanger the test-article, the cracks were allowed to grow and thus provide crack growth data as part of the damage tolerance testing. Wherever necessary, the cracked locations were strengthened in order to avoid cracking in production aircraft.

After the completion of the two lifetimes of fatigue testing, artificial flaws have been introduced by a very fine saw-cut or EDM at approximately 50 critical locations and damage-tolerance testing is under progress.

At the end of the damage-tolerance test, two residual strength tests, with the application of limit load and cabin pressurization of 10.5 psi, will be performed to the aircraft structure, in the presence of large cracks at several critical locations, including two-bay cracks. This will be followed by a selected teardown inspection.

11.3 STRUCTURAL INTEGRITY AND HEALTH-MONITORING OF COMPOSITE MATERIALS

11.3.1 Comprehensive Structural Integrity of Composites (Z. Granot, IAI and S. Gali, Consultant)

Composite structures must perform their function throughout the projected service life, while conforming to rigorous safety and economic requirements. The structures are subjected to various initial and in-service damage threats and are subjected to a realistic mix of load-time-environment sequences. In the ICAF 2005 National Review [1], an experimental and analytical program on the cumulative damage effects for repetitive loads in composites was discussed. In addition, a paper was presented at the ICAF 2005 symposium summarizing IAI's methodology for predicting the fatigue life of composite material structures [8].

Now this program is being expanded and generalized to consider not just repetitive load cycles, but also other factors contributing to the overall damage. The effects of load-time-temperature-moisture sequences including creep loading are all considered as contributing factors, both individually and collectively.

The tasks being considered are:

- Accelerated testing on various coupons and subassemblies, for both static and repetitive loading, and to various load-time-environment sequences
- Development of advanced modeling techniques to model and explain the behavior and failure modes of coupons and subassemblies
- Development and implementation of advanced failure criteria, for initiation, progression and final failure. These should consider static, fatigue, creep, environmental, and residual strength degradation
- Development of trade-off calculations for determining the most optimum materials and design features
- Development of advanced preventative, maintenance, monitoring and inspection techniques to enhance and maintain the structure through its service life

Expected results from the program:

- Accelerated testing techniques and know-how
- Advanced modeling techniques
- Advanced failure criteria and analytical methodology
- Analytical system for parametric trade-off studies
- Optimum design features
- Techniques for slowing degradation and life extension

11.3.2 Smart Bonded Composite Patch Repairs – Analysis and Testing (I. Kressel, IAI, S. Gali, Consultant, et al)

At the 2005 ICAF Symposium, a poster was presented on the damage tolerance of bonded composite repairs [9]. This work has been extended to include the "smart repair concept".

The recently introduced smart repair concept is aimed towards real-time assessment of repair integrity based on direct monitoring of internal strains, using embedded sensors. Methodology for establishing allowable defect size, based on extending existing analytical model, was numerically and experimentally verified. This methodology was also used for determining the minimal spatial resolution sensor net required for tracking the repair degradation over time. The expansion of defects such as patch debonds and crack in the metallic substrate were monitored by a low spatial resolution, optical Fiber Bragg Grating sensor net embedded in the composite patch. By correlating the optical Fiber Bragg sensors strain measurements with a numerical model, this sensing concept was able to identify and track damage propagation in real time with spatial resolution much better than that of the sensor net.

One of the important issues associated with bonded repairs is the presence of defects. Defects such as delamination or debonding may be generated during the bonded repair application or may develop during service. In order to assure the safe operation of the repaired structure, it is important to assess the repair integrity over time. This work presents experimental, analytical and numerical work aimed towards establishing acceptance criteria for bonded repair allowable defects. Special attention was given to the crack propagation rate of a cracked metallic structure, repaired by a composite patch with a debonded area over the crack. The effect of residual stress induced by the thermal expansion mismatch between the composite patch and the metal substrate was also considered.

The analytical model used for crack growth prediction is based on the Rose Model. This model predicts that the stress intensity factor of a crack in an isotropic material under a bonded patch repair will not change as the crack grows. Additional analytic evaluation, based on the Rose model, predicts that this result is also valid in the presence of a modest patch debond defect over the crack. Finite-element analysis is being performed, in order to verify these results.

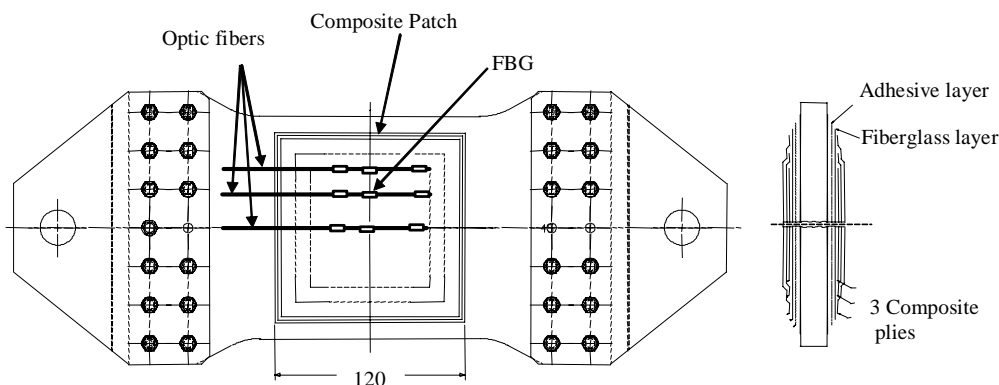
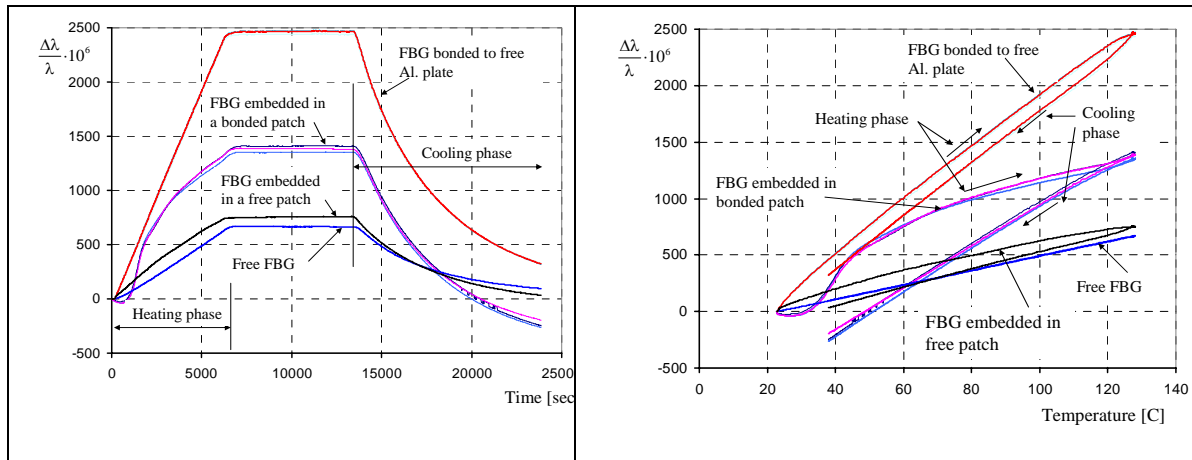


Figure 13: Smart Patch Specimen: Double Sided Bonded Repair Specimen with Embedded FBG.

Test specimens simulating typical bonded repair deterioration associated with debonding and initiation of cracks in the metallic substrate were manufactured and tested. (See Figure 13) The specimens were subjected to constant amplitude cyclic tensile loading (110MPa) at room temperature and elevated temperature of 70°C combined with 100% relative humidity. Crack length and debond size were inspected after each block of 25,000 cycles, using X-ray and ultrasonic inspections. Embedded defect expansion was also monitored using the FBG sensor net. Measurements were taken of changes in the strain field induced in the composite patch by both the growing crack in the metal substrate and patch-to-substrate debonds. By correlating these strain measurements with a numerical model, this sensing concept was able to identify and track damage propagation in real time with spatial resolution much better than that of the sensor net.

A nearly constant crack growth rate was observed for all the repaired specimens, with or without defects, as is expected by the FE analysis. The crack growth of a specimen having a debonded area, however, was higher

compared to a similar specimen without a defect. All the tested specimens demonstrated a slow crack growth rate, compared to an unrepaired reference specimen. It is concluded that the bonded repair concept has demonstrated slow crack growth rate in the presence of debonds.



(a)

(b)

Figure 14: (a) FBG Readings as a Function of Time, (b) FBG Readings as a Function of Temperature

The good correlation between the predicted damage, as derived from the FBG readings, with the conventional non destructive inspections makes such sensing concept an excellent candidate for bonded repairs structural health monitoring system. Figure 14 shows the FBG readings during the cure cycle, as a function of time and temperature.

The results of the study will be presented as a poster at the ICAF 2007 Symposium [10].

11.3.3 Damage Detection in Composite Materials (P. Pevzner, A. Berkovits et al, Technion)

Techniques which use embedded optical fibers in composite structures are considered to be very promising for non-destructive detection of damage. The notion of “smart” structures has become commonly used for such structures. In addition to measuring the response of a composite structure to external stimuli, embedded fiber optic sensors would make ideal “nerves” for sensing the local integrity of such structures.

A new approach for damage detection in composites, employing heat “leakage” from cracked or broken optic fibers embedded in or bonded to composite plate structures, was proposed and investigated. Optic fibers that were stripped of their jacket and weakened were embedded in or attached to a composite plate structure, so that they cracked when cracks or delaminations occurred in the composite. It is shown that, at the location of a crack in a fiber, transmitted light energy was converted into heat energy causing the temperature in the neighborhood of the crack to rise. The temperature change was detected by an infrared camera.

An advantage of the proposed method is that it can exploit optic fibers which have already been embedded into a structure for other purposes, such as strain, temperature and frequency measurements. In other cases, fibers can be bonded to the rear surface of existing structures. In this way the sensors can also be easily replaced when damaged. Experiments supplemented by theoretical studies were carried out. In the experiments, an impacted damaged graphite-epoxy plate showed that the heat energy emitted by fibers bonded to a composite plate was adequate to change the local temperature, so that it could be accurately identified by an infrared camera. (See Figures 15 and 16.) The size of the damage, which can be detected by this method, depends on the density of embedded optic fibers, distance of the fibers from the surface, and the laser power.

The results of this study were presented at the 47th Israel Annual Conference on Aerospace Sciences [11].

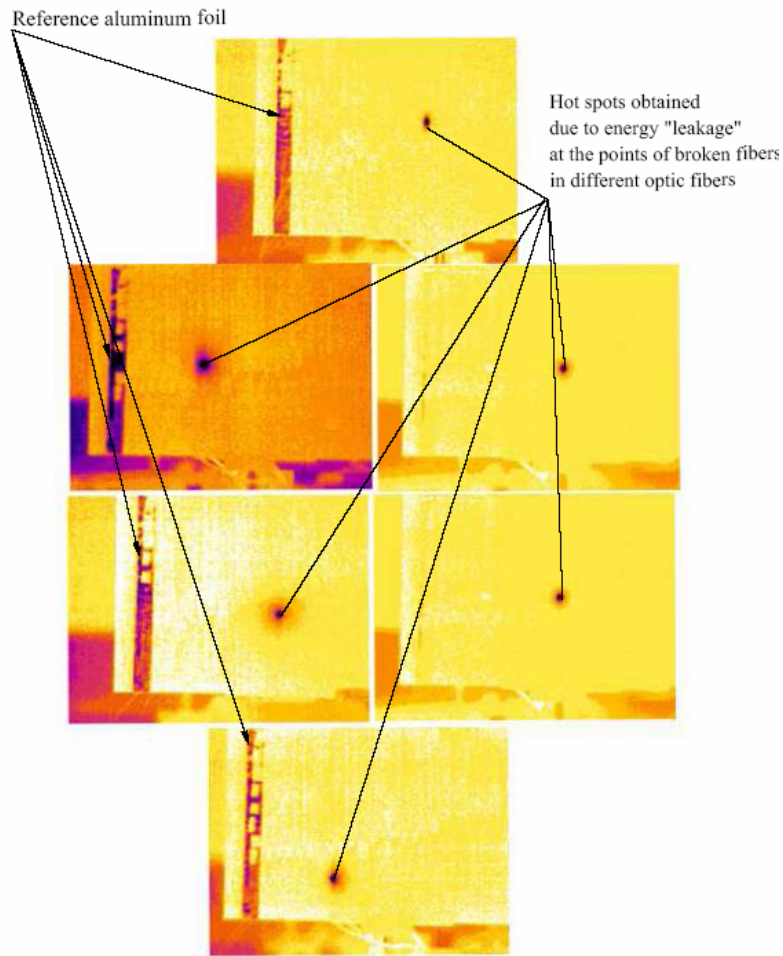


Figure 15: Typical pictures obtained by the infrared camera for different broken fibers.

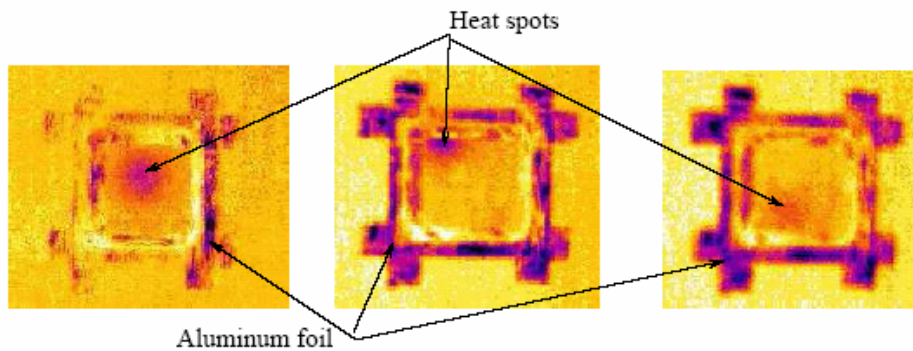


Figure 16: Infrared camera pictures of heat spots on the rear surface of a composite plate.

11.3.4 Structural Health Monitoring for Composite Structures Based on Lamb Wave Detection (P. Botsev et al, Tel Aviv University; I. Kressel et al, IAI and S. Gali, Consultant)

The concept of Structural Health Monitoring (SHM) is aimed towards real time structural integrity assessment using a network of embedded sensors. In the aircraft industry, for example, airworthiness requirements are currently maintained by extensive inspection programs and the adoption of the SHM concept may reduce inspection downtime and over-all maintenance cost.

A very attractive method for detecting and monitoring damages in composite or metal structures employs ultrasonic Lamb waves. Lamb waves can be generated with relatively small piezoelectric actuators by means of a pulse with a known Fourier transform. In the low frequency range it is possible to generate only flexural waves. The interaction of the generated flexural waves with a defect induces an echo signal, which can then be detected, normally via piezoelectric sensors, and electronically processed. The energy produced by this echo signal has a strong correlation with the size of the damage and may be used to follow its evolution. Lamb wave techniques can also determine damage location. Since Lamb waves can propagate over relatively long distances, this technique is especially useful for interrogating large structures. However, one of the major disadvantages of using piezoelectric transducers is the need to wire each sensor and protect against electromagnetic interference. In principle, fiber optic sensors, and in particular fiber Bragg gratings (FBG) appear to be excellent candidates to replace piezoelectric sensors as ultrasonic detectors (and even actuators) due to their high sensitivity to mechanical strain, small size, immunity to electrical interference and capability of dense multiplexing. Moreover, for composite structures, such optic fibers sensors can be easily embedded into the structure, eliminating the need for sensor protection, and can be used to monitor also strain and temperature during curing or service.

In this work, our independent studies of low frequency ultrasonic Lamb wave detection using embedded standard (SMF) FBG sensors in composite structures are reported. Not only has good correlation has been obtained among the readings of both surface-attached and embedded FBGs and the output of a co-located piezoelectric sensor, but we have also characterized the directional sensitivity of the sensors and studied the dispersive nature of the Lamb-wave. Since flexural Lamb waves are quite dispersive, it is difficult to accurately evaluate time-of-flight characteristics and their dependence on surface and internal damage and defects, without the ability to compensate for the dispersion of the acoustic wave. Finally, the embedded FBG sensor was used to identify and locate a damaged area on the composite structure. A typical result is shown in Figure 17.

The results of this study were presented at the 47th Israel Annual Conference on Aerospace Sciences [12].

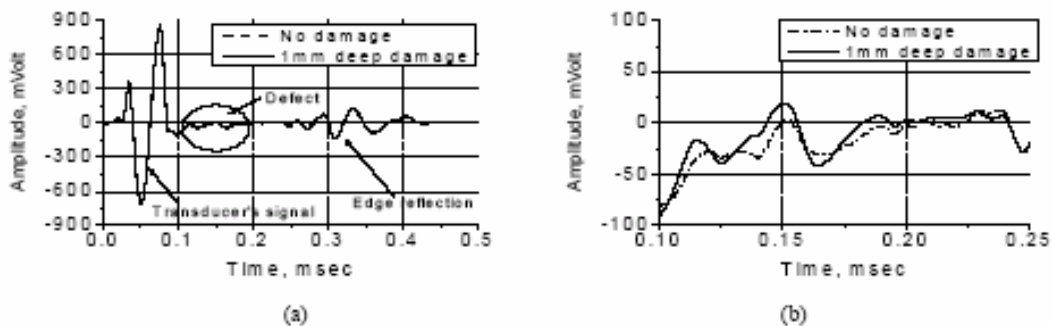


Figure 17. Crack detection in composite plate: (a) measured signal, (b) zoom of signal

11.4 PROBABILISTIC STUDIES

11.4.1 Evaluating Probability of Second Layer Detection by Using Low-Frequency Eddy-Current NDI (C. Matias, A. Brot and W. Senderowits, IAI)

Aircraft structures, designed and certified to the damage-tolerance requirements, must be inspected periodically for cracks. These inspections usually result in significant aircraft downtime and may be expensive to implement. In order to reduce the cost of inspections, without compromising aircraft safety, the use of low-frequency eddy-current (LFEC) non-destructive inspection (NDI) techniques is being investigated, and was previously reported in the 2005 Israel National Review [1]. Since the previous review, additional test data was supplied by the Israel Air Force, whose inspectors performed LFEC measurements using the test rig described below.

Crack detection by means of high-frequency eddy-current (HFEC) non-destructive inspections for an uncovered layer (first layer) is widely used, thoroughly investigated and well established in the aircraft industry. That technique has an extensive statistical database, and a reasonably accurate, well-correlated Weibull three-parameter statistical model of crack detection probability. On the basis of that model and the results of tests conducted in the framework of this study, statistical parameters were set in order to establish probabilities of detection correlations to the LFEC NDI.

A test program was conducted in order to examine the LFEC capability of crack detection. A 7075-T7351 base-plate, with crack sizes varying from 2.5 to 12.7mm, was installed beneath 7075-T7351 cover plates having a thickness ranging from 1.0 to 6.35mm. The base-plate has 100 holes, from which 30 of them have a crack that emerges out of the hole. The 30 cracked holes are randomly arranged. The cracks appear at five different lengths, and at different orientations, which are of typical for in-service inspections. The cover plates are of six different thicknesses, containing 50% plain holes and 50% countersunk holes. The inspections are being performed around the holes, in the presence of HI-LOK fasteners. These features are of typical structural aircraft details and of typical in-service inspections. Inspectors performed the LFEC inspections, using their own instruments and methods (probes, oscilloscopes, calibration etc.). In order to maintain an objective test, the holes were numbered and the cover plates were rotated relatively to the base-plate for each test differently, so that the inspector will not be aware of the specific crack locations.

It was shown that a correlated Weibull distribution can be used to express the crack detection probabilities, for the LFEC NDI, as a function of crack length and cover plate thickness, based on the statistical data gathered at the tests done in this study. (See Figures 18 and 19)

In this way, a statistical model that will predict the probability of crack detection as a function of crack length and cover plate thickness was established. This will allow the use of the LFEC NDI technique with a relatively high degree of reliability for rationally determined inspection intervals. These inspection intervals will be significantly longer than those determined by alternate inspection methods for hidden cracks.

The results of this study were first presented as a poster at the ICAF 2005 Conference. Since then, the results were updated, based on additional test data that was obtained. The updated results were presented at the 2006 USAF Aircraft Structural Integrity Program Conference [13].

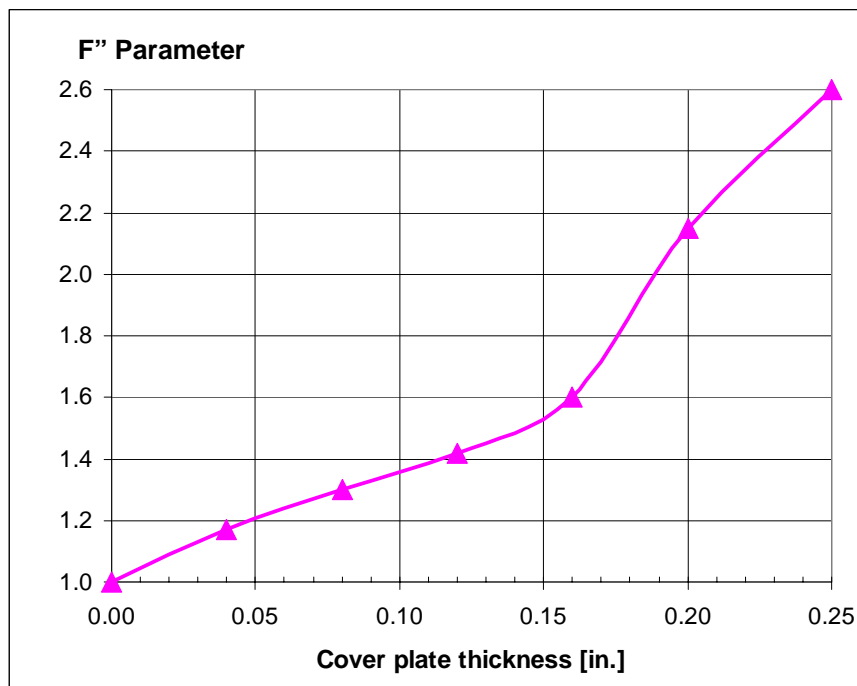


Figure 18: Detectable Crack Size Factor as a Function of Cover Plate Thickness ($F = \text{LFEC detectable crack size divided by the HFEC detectable crack size}$)

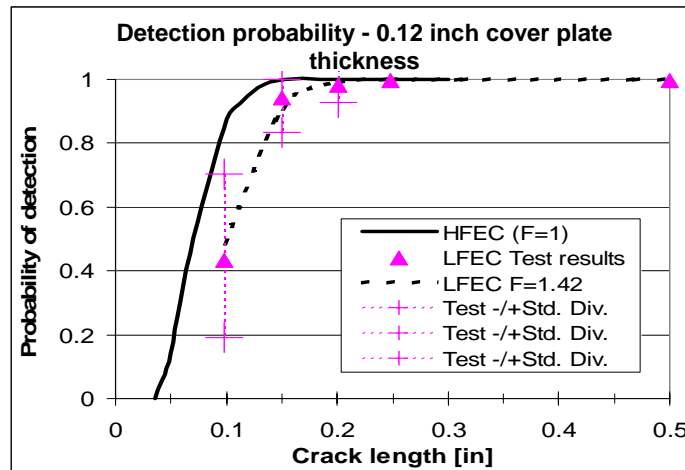


Figure 19: Typical Probability of Detection Result for LFEC Inspection

11.4.2 Fatigue Life Estimation Reliability (Y. Rabinowicz and Y. Roman, Hebrew University of Jerusalem)

Fatigue life estimation reliability is being investigated by means of probabilistic fracture mechanics methodology in order to determine, and better understand, the significance of variability in reported fatigue crack propagation rates. The aim is to improve the reliability of fatigue life estimation by modeling fatigue crack propagation in a more realistic way. This activity has recently begun, and the specific results of the study will be reported at the next Israel National Review.

11.5 MISCELLANEOUS

11.5.1 Stress Intensity Functions in the Neighborhood of Edges in a Three-Dimensional Linear Elastic Body (Z. Yosibash, N. Omer, et al, Ben-Gurion University)

This research is a continuation of previous work presented in the 2005 Israel National Review [1].

The computation of stress intensity functions in the neighborhood of edges in a three-dimensional linear elastic body is of major importance in engineering practice, and some methods for extracting these from finite element solutions have been earlier proposed. However, a detailed mathematical framework of the 3-D edge singularities seems not to be available, and the methods are not the most efficient and accurate due to the need of extracting the Edge Flux Intensity Functions (EFIFs) very close to the edges. Towards developing efficient and accurate methods, we first show in [14] that the commonly used J-integral in 3-D (which becomes a path-area integral) for the extraction of *pointwise values* of the ESIF is indeed path-independent. Nevertheless, it is inefficient because of the need to include the singular edge in the computational domain.

Towards developing efficient and accurate methods, the asymptotic solution of elasticity problems, in the vicinity of edges in 3-D isotropic and anisotropic domains is provided explicitly in [15]. It involves a sequence of eigenpairs and their corresponding coefficients which are functions along the edge. These are of high engineering importance because failure theories involve them. The determination of the eigenpairs (and more importantly their shadows), and reliable computation of the coefficients (edge stress intensity functions - ESIFs) of the asymptotic expansion are addressed in [15, 16]. Special attention is devoted to the numerical methods and to the efficiency and reliable computation of the eigenpairs and extraction of ESIFs. Anisotropic domains and multi-material interfaces typical to composite materials of practical engineering importance are addressed. As an example we present in Figure 20, the functional representation of the ESIF for a compact tension specimen along the crack front extracted by the quasilocal function method (dotted line), the pointwise J-integral and the 2-D plane strain approximation. One may notice that the crack front (right picture in Figure 20) is indeed curved according to the ESIF.

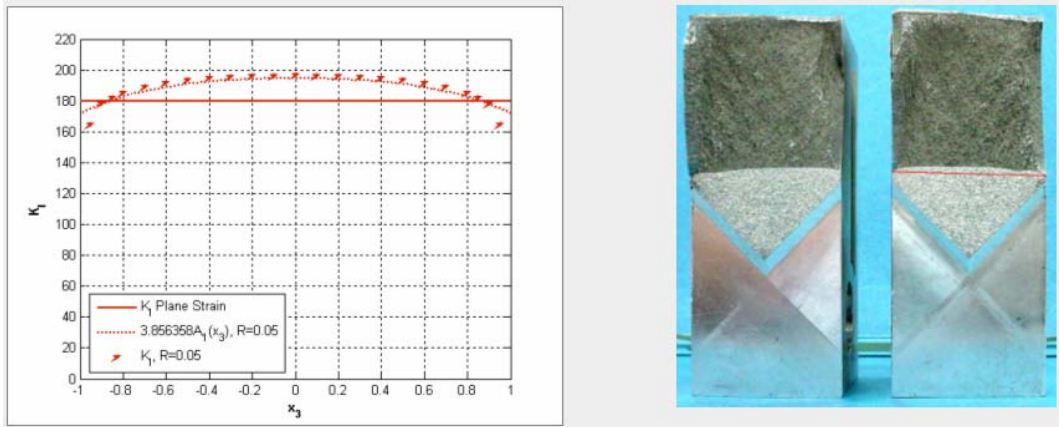


Figure 20: Functional Representation of the ESIF for a Compact Tension Specimen along the Crack Front Extracted by the Quasidual Function Method

11.5.2 Linear Elastostatic Problems in the Vicinity of Reentrant Corners (Z. Yosibash, E. Priel et al, Ben-Gurion University)

This research is a continuation of previous work presented in the 2005 Israel National Review [1].

A research project reported in [17] and [18] is directed to solutions of linear elastostatic problems in the vicinity of reentrant corners subject to mixed mode loading and the formulation of a failure criterion for these problems. Brittle elastic components containing V-notches fail at significantly lower loads than the material strength would suggest.

In the past 10 years, failure criteria for such components under mode I loading have been proposed and validated by experiments. For a more realistic mixed mode loading the number of failure criteria is much smaller and no agreement exists in the scientific community on the “best criterion”. During the past 2 years three new mixed mode failure criteria for brittle elastic V-notched components were investigated [18], two of which are generalizations of known mode I failure criteria and the third is being introduced for the first time.

To validate the criteria, mixed mode loading experiments on PMMA and MACOR (glass ceramics) V-notched bar specimens were conducted. The parameters that govern failure initiation were computed by the p-version of the finite element method (p-FEM) from models representing the experimental specimens. The p-version FE analyses for the prediction of failure loads are outlined and results comparing prediction to experimental observations are presented. A typical example of a V-notch specimen, its p-version FE model and the predicted vs. experimental failure load for several mode-mixity values, is shown in Figure 21.

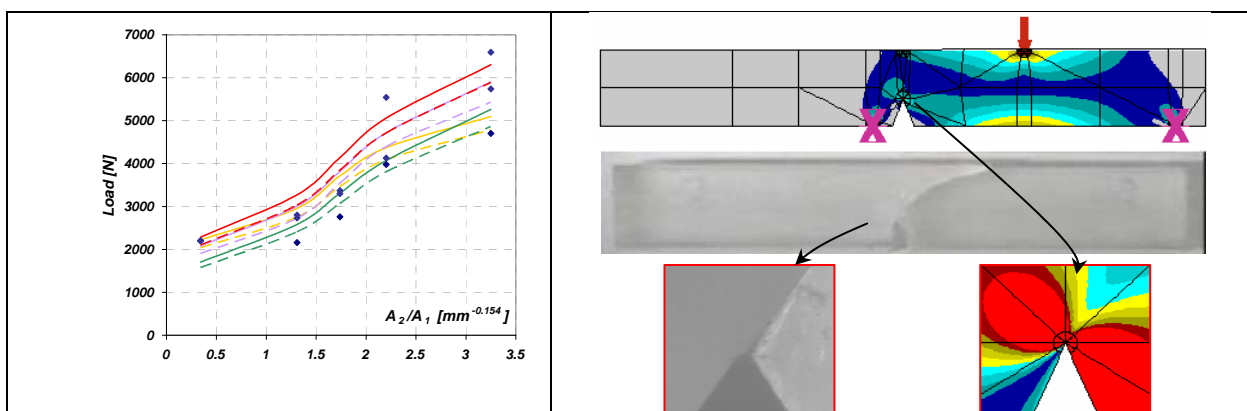


Figure 21: p-version FEM of a V-Notch Specimen and the Predicted vs. Experimental Failure Load for Several Mode-Mixity Values

11.5.3 Cracks in Anisotropic Materials and Delamination in Fiber Reinforced Composites (L. Banks-Sills, Tel-Aviv University)

The previous Israel National Review [1] reported about research being performed at the Dreszer Fracture Mechanics Laboratory at Tel-Aviv University. During the last two years, investigation of the behavior of cracks in anisotropic material has been carried out. In addition, the effect of crack face contact and friction was examined numerically for the bimaterial Brazilian disk specimen. Finally, fracture toughness tests have been performed on specimens containing a crack along the $+45^\circ/-45^\circ$ interface of fiber reinforced composite materials.

Reference [19] is a continuation of the investigation begun in [20]. In these investigations, the conservative M -integral for mode separation was extended for cracks in anisotropic material. The crack coordinates were defined as x , y and z ; whereas, the material coordinates were x_i , $i = 1; 2; 3$. In Part I [20], the x_3 -axis was aligned with the z -axis and $x_3 = 0$ was taken as a plane of material symmetry. In Part II [19], the general anisotropic problem was considered; that is, the crack plane was at an arbitrary angle to the material directions or the most general anisotropic material was used. A three-dimensional treatment is required for this situation in which there may be two or three modes present. A three-dimensional M -integral was extended to obtain stress intensity factors. It was applied to several test problems, in which excellent results were obtained. Results were found for a Brazilian disk specimen made of isotropic and cubic materials. Two examples for the latter were examined with material coordinates rotated with respect to the crack axes.

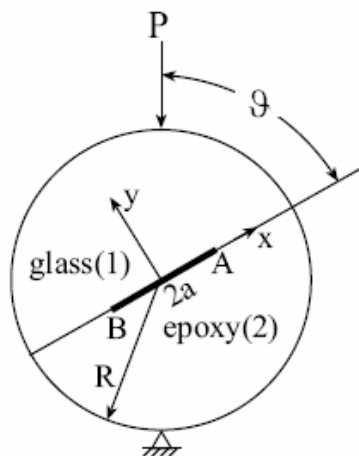


Figure 22: A Brazilian disk specimen subjected to a concentrated force at loading angle ϑ

The effect of crack face contact and friction on Brazilian disk specimens was studied in [21]. This is a continuation of the study in [22] where the elastic two-dimensional problem of contact with friction was formulated and solved by means of a finite difference method. In [21], a full curvilinear transformation was employed to study the effect of contact and friction on Brazilian disk specimens containing a crack and subjected to concentrated loads at angles $0^\circ < \vartheta < 90^\circ$ (see Fig. 22). Homogeneous and bimaterial disks made of glass and epoxy were considered. The effect of loading angle and friction coefficient on the stress intensity factors, as well as the contact length was studied. Results were compared to available semi-analytical and finite elements results. It was found that when the crack faces are in contact without stick zones, an increase in friction causes a decrease of the normal gaps, tangential shifts and stress intensity factors. When stick conditions appeared in the contact zone, an increase in the coefficient of friction also resulted in increasing the stick zone within the contact zone. As an example, the normal gap ΔU_y and tangential shift ΔU_x for loading angle $\vartheta = 25^\circ$ and friction coefficients $\mu_f = 0, 0.25, 0.5, 0.75$ and 1 are plotted in Figs. 23a and 23b, respectively. It may be observed that the normal gap and the absolute value of the tangential shift decrease and the contact zone increases as the coefficient of the friction increases.

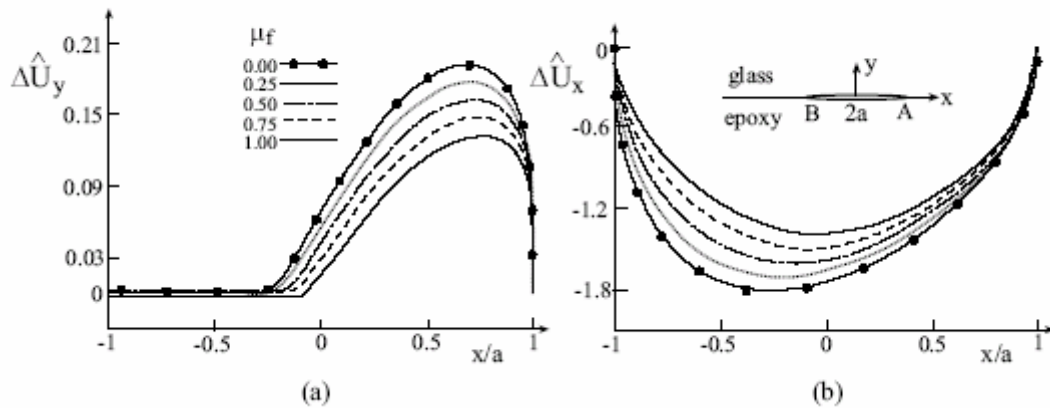


Figure 23: Effect of friction on the (a) normal gap and (b) tangential shift of a glass/epoxy Brazilian disk specimen with normalized crack length $a/R = 0.5$ and loading angle $\theta = 25^\circ$

Another project which was worked on for several years, involves predicting delamination in fiber reinforced laminate composites. Two interfaces have been considered: $0^\circ/90^\circ$ and $+45^\circ/-45^\circ$. The latest results are experiments which have been carried out to determine the delamination toughness for a crack along the interface between two transversely isotropic materials in the $+45^\circ/-45^\circ$ -directions [23]. The material chosen for study consisted of carbon fibers embedded within an epoxy matrix. A crack was introduced between two layers of this material, with fibers in the upper layer along the $+45^\circ$ -direction and those in the lower layer along the -45° -direction, both with respect to the crack plane. Brazilian disk specimens shown in Figs. 24 were employed in the testing. Laminates made from graphite/epoxy (AS4/3502) prepregs were cured in an autoclave at a high temperature and pressure. As a result, residual stresses were induced within the laminate. A plate approximately 12.4 mm thick was fabricated by Israel Aerospace Industries with 15.4 mm wide and 25.4 μm thick Teflon (FEP fluorocarbon resin) strips introduced periodically between two of the $+45^\circ/-45^\circ$ layers. The plate consisted of an inner part of $\{0, -45, +45, 0\}_s$, each of nominal thickness 0.54 mm. Outer stiffening layers of $\pm 45^\circ$, 4.05 mm thick were added to prevent plate bending. Strips were cut from the plate to form the specimen illustrated in Figure 24.

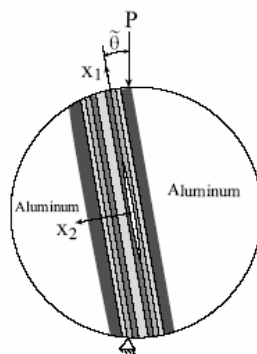


Figure 24: Brazilian disk specimen containing a composite strip with a crack along a $+45^\circ/-45^\circ$ interface

To calibrate the specimens, stress intensity factors were obtained which result from the applied load, as well as residual curing stresses. It may be noted that all three modes are coupled, leading to a three-dimensional problem. The finite element method and a mechanical M -integral were employed to determine the stress intensity factors arising from the applied load. For the residual stresses, a three-dimensional conservative thermal M -integral was presented for stress intensity factor determination. The stress intensity factors found for the applied load and residual stresses were superposed to obtain a local interface energy release rate G_I , together with two phase angles ψ and ϕ .

From the load at fracture, the critical interface energy release rate or interface toughness G_{Ic} as a function of phase angles was determined and is exhibited in Fig. 25. For each specimen, 21 points along the crack front are shown as round symbols. The surface was obtained as a fracture criterion. Points along the crack front for 19 of the specimens intersect the surface. It may be postulated, for these specimens, that some of the points along the crack front have become critical and drag the rest of the crack front with them as the delamination expands. For

two of the specimens, all of the points are above the surface; whereas for five of them, all of the points are below. This behavior is considered as experimental scatter.

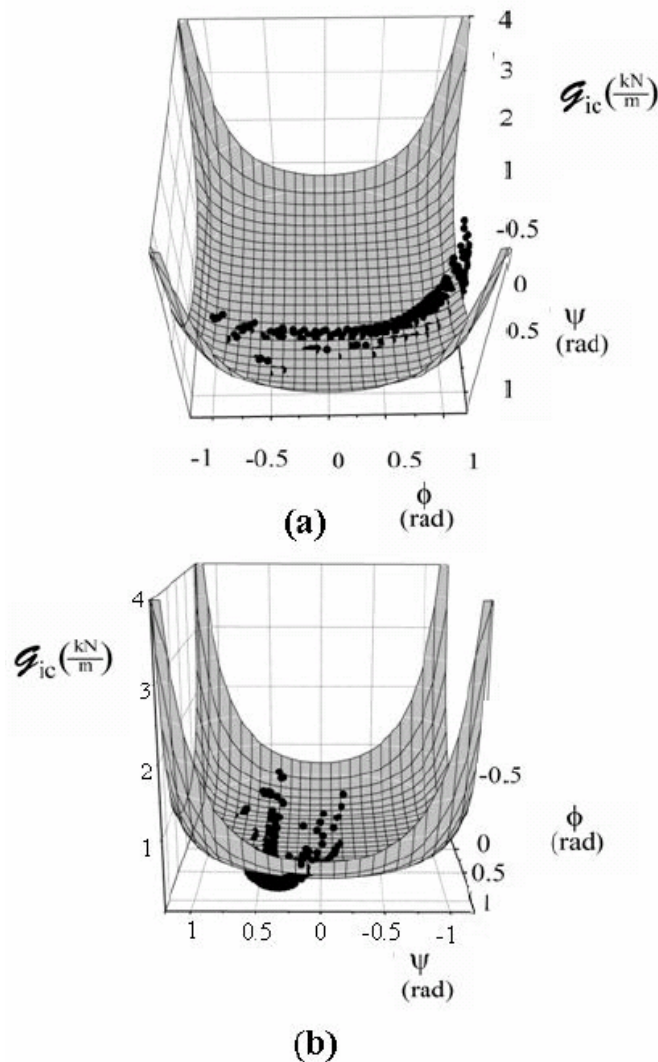


Figure 25: Delamination toughness G_{ic} along a $+45^\circ/-45^\circ$ interface as a function of mode mixity ψ ($L = 200\mu\text{m}$) and phase angle ϕ for graphite/epoxy (AS4/3502). The criterion is seen as the surface.

The surface in Fig. 25 may be used to predict failure. Consider a structure which has a delamination in which the fibers in the upper layer are in the $+45^\circ$ -direction and those in the lower layer in the -45° -direction. A safe situation is one in which all of the points along the crack front have G_{ic} values below the surface for their corresponding phase angles. Of course, similar to the $0^\circ/90^\circ$ interface [24], there is scatter in the results and, hence, a statistical analysis should be carried out.

11.5.4 Crack Detection, Without Remeshing, Using a Genetic Algorithm (D. Rabinovic and D. Givoli, Technion)

A new computational tool is being developed for the accurate detection and identification of cracks in structures, to be used in conjunction with non-destructive testing of specimens. It is based on the solution of an inverse problem. Based on some measurements, typically along part of the boundary of the structure, that describe the response of the structure to vibration in a chosen frequency or a combination of frequencies, the goal is to estimate whether the structure contains a crack. If so, the goal is to find the parameters (location, size, orientation and shape) of the crack that produces a response closest to the given measurement data in some chosen norm.

The inverse problem is solved using a genetic algorithm (GA). The GA optimization process requires the solution of a very large amount of forward problems. The latter are solved via the extended finite-element method (XFEM). This enables one to employ the same regular mesh for all the forward problems. Performance of the method is demonstrated via a number of numerical examples involving a cracked flat membrane. Various computational aspects of the method are discussed, including the a priori estimation of the ill-posedness of the crack identification problem. Figure 26 describes the operations involved in the genetic algorithm. Figure 27 presents solution fields for two crack orientations.

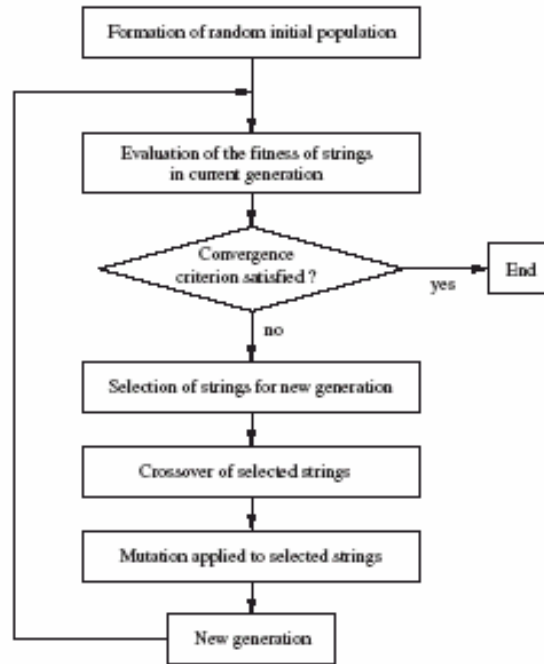


Figure 26: Operations Involved in the Genetic Algorithm

This scheme is being currently extended in several directions. Among them are the use of *time-dependent* impulse response data, which is quite common in geophysics, for example, due to the great importance of the arrival time information, *two- and three-dimensional elastodynamics*, and special procedures for measurements containing *noise*. Regarding the latter issue, when noise is present in the measurements and is magnified by the inverse operator, the resulting error in the solution of the forward problems may hamper detectability. Special filtering schemes may be needed to overcome this difficulty. Future work will also hopefully include crack configurations which are closer to industrial practice, including the important case of three-dimensional cracks. In addition, the proposed method will be applied to other types of identification problems, not necessarily involving cracks.

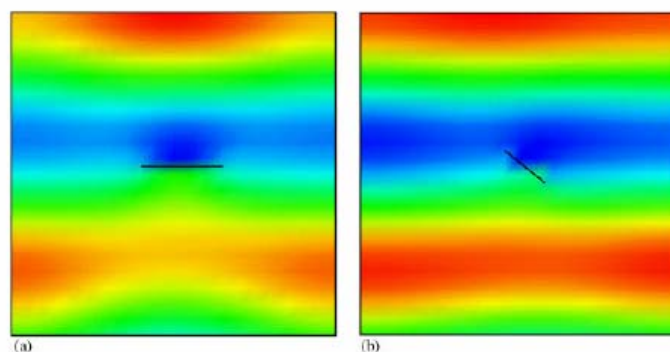


Figure 27: Solution Fields for Two Crack Orientations: (a) Horizontal Crack; (b) Crack with 45° Orientation.

The results of this study were presented at the 47th Israel Annual Conference on Aerospace Sciences [25] and will be published in [26].

11.5.5 Health Monitoring of Structural Joints (B. Karp, D. Rittel and D. Durban, Technion)

Condition-based real-time maintenance of structural components is a relatively new area, enabling cost-effective maintenance and improved functional reliability of the structure. Emergence of this field has been enabled by intensive developments of structural health monitoring (SHM) systems during the last few decades. Basically, SHM systems consist of a physical device for data collection and a signal processing computer along with an appropriate algorithm. Efficient identification of the onset of damage, or deterioration, at the earliest possible stage, centers on the sensitivity of a selected diagnostic parameter of structural response to the type of damage to be detected. That sensitivity is reflected in the design of the monitoring device and in the selected signal processing algorithm.

Currently, SHM systems rely mainly on three diagnostic parameters considered as structural markers: modal properties of vibrating structures, propagation of Lamb waves, and impedance of the structure as sensed by attached PZT wafers. It has been recently suggested the use of modal damping ratios as another marker for monitoring single-lap adhesive joints. Experiments reveal that the sensitivity of this method is favorable in comparison with frequency-based methods.

This research reports on a feasibility study for employing *end effects* as an alternative diagnostic parameter (structural marker) for health monitoring of structural joints. In a sense, these end effects can be considered as a special case of Lamb waves spectra. Nevertheless, *propagating waves* are dominant in the design and analysis of existing SHM methods, whereas the emphasis here is on end effects associated with *evanescent waves*.

The proposed methodology is based on the known observation of high sensitivity of the *near field* to details of end data. Evanescent waves are generated at the ends of waveguides due to spatial incompatibility between the end data and the propagating modes. Under static loading, this pattern falls under the study of Saint-Venant's principle. Under dynamic loading, although no agreed upon analogy to the static Saint-Venant principle has yet been found, that sensitivity has been observed in problems related to waveguides. Traditionally, both in statics and in dynamics of structures, reliance on the response of the structure within the near field has not been of practical interest. Here, it is indeed this sensitivity to end data that is taken advantage of. End effects are regarded as the joint signature and contain key data pertaining to the integrity of edge fixation. To investigate in laboratory tests the effect of damaged end conditions on near field effects, a cantilever beam with controlled damage of the clamping conditions was chosen.

Dynamic response of a cantilever beam has been experimentally examined to demonstrate near field sensitivity to details of end conditions. "End conditions" are perceived here as a manifestation of the details of the joint, with possible deviations from the designed original configuration. In view of the analytical similarity between static and dynamic end effects (exponential decay in axial direction), both static and dynamic experiments were performed. In the static experiments a weight was attached to the free end of the beam. In the dynamic experiments a short rod was dropped to hit the same free end of the beam. Strains along the centerline of the beam were measured for repeated identical excitations with (controlled) different clamping conditions of the built-in end. Five strain gauges were attached to the upper surface of the beam, three located within the immediate vicinity of the clamped end (near field) and two at a distance from it (far field).

Clamping of the beam is realized by six screws. Various combinations of tightness of the screws were considered as simulating different clamping conditions. It is noted here that "clamping" is a term used in practice with no definite meaning within the theory of elasticity. For the purpose of the present work, the phrase *clamping condition* will be used to discriminate between various ways in which end fixation is realized, all of which could be considered as "clamping" for practical engineering purposes. Various levels of screws' tightness can be regarded as different end conditions and as artificially induced damage to the joint, simulating events such as loosening of bolts, debonding, cracking, or loss of rivets. Recalling the axial decay of eigenfunctions in static fields, and the existence of evanescent waves in dynamic response, it is expected that at least part of the strain history readings will reflect the controlled changes in *clamping conditions*. Figure 28 shows some experimental results obtained in this study.

The main result emerging from this study is that simple experimental techniques, along with monitoring surface strains in the near field, enable the identification of even minor changes in the joint condition. In the static experiments the condition of completely and partially loose screws was identified. In dynamic experiments completely loose screws were identified clearly with less conclusive results for partially loosened screws. These observations agree well with the analysis of end effects given found in the literature. In both static and dynamic experiments, the far field measured data of strains was found to be insensitive to fine details in the *clamping condition*.

The results of this study were presented at the 47th Israel Annual Conference on Aerospace Sciences [27].

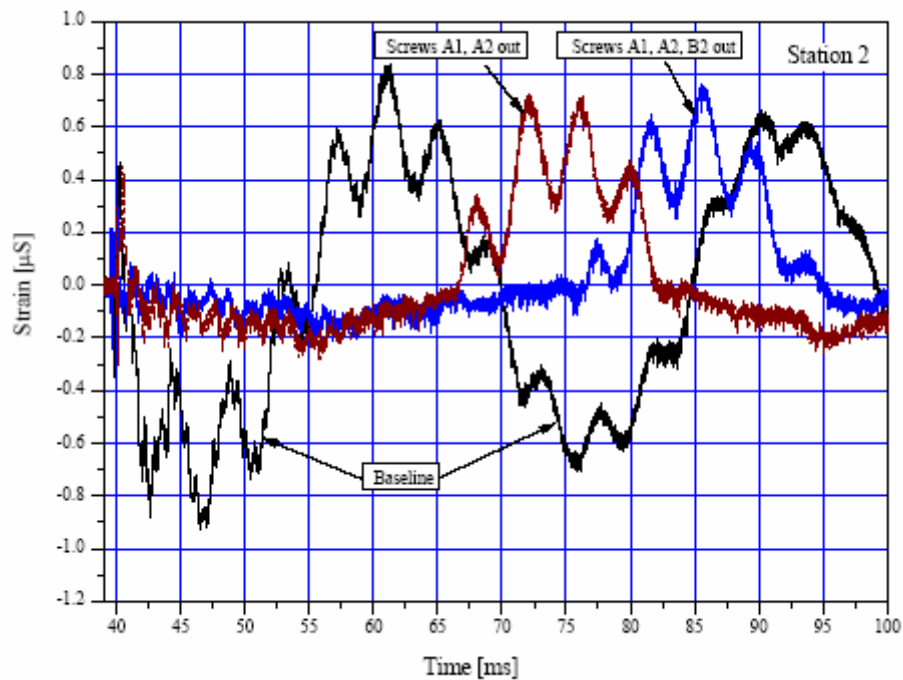


Figure 28 – Measured Strain for Three Clamping Conditions with More Than One Screw Missing

11.5.6 Fleet Usage Spectrum Evaluation and Mission Classification (M. Ben-Noon, et al, IAF)

Safety and economical considerations lead to advanced maintenance approaches that are based on identifying individual aircraft maintenance needs. A major aspect of structural maintenance is related to accumulated fatigue damage that depends on the actual usage of the aircraft. Some Fleet Structural Maintenance Plans (FSMP) use Individual Aircraft Tracking (IAT) programs that are based on tracking the actual usage of each aircraft. Various methods such as G counting and accumulation of mission types or flight regimes are used to track and reflect actual individual usage of each aircraft in a manner that will allow individual fatigue damage accumulation.

Advanced fatigue monitoring systems use recorded flight data in various forms (G counters, maneuver data, strain gauge data, etc.) and formats (exceedances, time-history) for fatigue damage accumulation. These systems are mostly used on fighter aircraft fleets. Cargo and helicopter fleets base their tracking systems on pilot reports that define the mission type per sortie. Advances such as installing flight data recorders on cargo fleets provide an opportunity for automated data collection.

One of the tasks required in most IAT systems is mission classification, which is used to accumulate damage per mission or to choose pre-studied crack growth curve. The former approach is common for cargo and transport aircraft (mission-by-mission integration), while the latter is used in the strike fighter fleets (damage parameter integration).

In the mission-by-mission integration method, the fleet manager will have to pre-identify the typical missions in the usage spectrum to perform the fatigue analysis for each control point and each mission type. The fatigue monitoring process for damage integration uses this database and pilot log data that identifies each sortie with predefined mission type. The advantage of the mission-by-mission integration method is its simplicity of damage accumulation. The disadvantages are the efforts exerted for analyzing each control point for all typical missions and the dependency on pilots' log that does not describe the mission adequately or comply with the predefined mission characteristics. This method was found to be most suitable for cargo and transport aircrafts because most of the load cycles are characterized by time in various altitude bands.

The damage integration method calculates damage based on correlation between the damage parameter and stress. To improve the accuracy of damage accumulation utilizing this method, some systems use the mission type data (e.g. different types of air-to-air missions).

From IAF's experience, IAT systems based on pilot questionnaires and pilot log data are not reliable. The predefined squadron missions are built from a combination of several sub-missions that are not consistent. The IAT system, which is based on the approach that tracks missions rather than sub-missions, reduces the accuracy since only a few missions enter the predefined combinations. Furthermore the pilot reports are subjective and inconsistent because of the difference between the predefined missions and the actual missions flown.



Figure 29: A C-130 Aircraft Flown by the Israel Air Force

To overcome these difficulties the IAF decided to take a step towards a fully automated Fleet Usage Spectrum Evaluation (FUSE) and Aircraft Mission Classification (AMC) system that will replace pilot reports. Installation of Crash Data Recorders (CDR) on the IAF C-130 fleet in recent years opened the door to Individual Aircraft Tracking (IAT) based on recorded and reliable operational data. Results show that it contributes to flight safety, reduction of maintenance costs and assists in the investigation of structural damages. The IAF management defined the support of advanced fatigue monitoring plans, by extracting data accumulated in the digital data record systems, as a major task. The first step was a "proof of concept" of the development of a mission recognition system based on C-130 CDR data, which would be used as input to the current IAF C-130 fatigue system. Figure 29 Shows a C-130 Aircraft in the IAF fleet. Figure 30 describes the C-130 IAT system with FUSE and AMC replacing pilot reports.

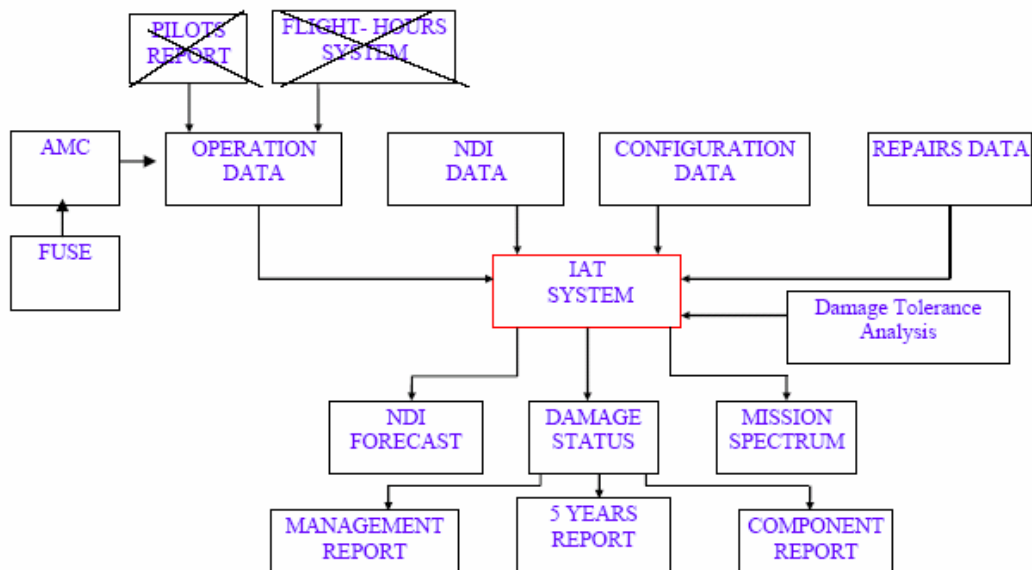


Figure 30: The C-130 IAT System Showing FUSE and AMC Replacing the Pilot Reports

The automatic FUSE process was used to create the IAF C-130 mission spectrum out of a 4800 sortie time-history that resulted in 50 sub-missions (clusters). Examination of the sub-missions in each cluster shows that the process is successful in grouping similar (but not necessarily identical) missions. Figure 31 describes the noise-reduction and smoothing process used to process the signals.

Automatic Fleet Usage Spectrum Evaluation and Aircraft Mission Classification, based on a pattern recognition approach, were developed and demonstrated on the C-130 IAF fleet. The performance of the system is strongly dependent on each of the basic modules, where feature quality is the most significant.

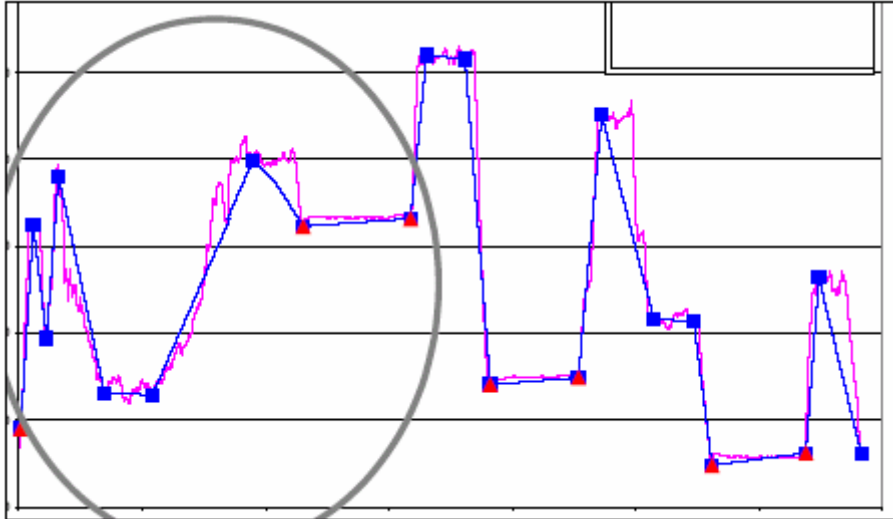


Figure 31: Transformation of a Noisy Signal into a Segmented Signal

The FUSE and AMC modules developed under this project can be used for any IAT system that is based on the mission integration method. The FUSE and AMC modules can also be useful for mission typing in IAT systems that are based on the damage parameter integration

Mission classification can also be used as the first step towards implementation of the IAT approach in rotary wing fleets, in order to calculate the added damage per mission. It seems reasonable to prefer regime recognition that is based on maneuver classification, but it requires much greater effort to accomplish.

The results of this study were presented at the 2006 USAF Aircraft Structural Integrity Program Conference [28].

11.5.7 Lessons Learned from Historical Aircraft Accidents (A. Brot, IAI)

This topic was presented at the 46th Israel Annual Conference on Aerospace Sciences [29]. It is based, in part, on previous work performed by Tom Swift, Jaap Schijve, Anders Blom and Bob Eastin.

During the last half-century, dating back to the two Comet accidents of 1954, the process of designing aircraft to fatigue life requirements has evolved from *nearly non-existent* rules to an extensive set of *fatigue and damage-tolerance regulations*. These regulations apply today to both the military and civilian sectors of aircraft design. They apply to both new designs and aging fleets, and apply to modifications and repairs to existing aircraft. We can trace the development of many of the features of these regulations to five major accidents that occurred during the last half-century.

- The de Havilland Comet I was the first modern high-altitude, jet-propelled passenger aircraft. Its first flight was in 1949, and it entered passenger service in 1951. In January 1954, a Comet disintegrated in the air and crashed near the island of Elba. It had experienced only 1286 pressure cycles at failure.
- The F-111 fighter-bomber entered service with the USAF in 1968. It featured a “swing-wing” supported by D6AC steel pivot-fittings. In 1969, Aircraft 94 (F-111A) crashed while performing a low-level, 4g bombing run. It had flown only 107 flight-hours before the accident.

- In 1977, a Dan-Air B707-321C aircraft crashed at Lusaka, Zambia after the entire right-hand horizontal stabilizer separated in flight during the approach to landing.
- In 1988, a Boeing 737-200 aircraft, operated by Aloha Airlines, had a sudden failure of the upper portion of the fuselage at a 24,000 ft. altitude over the Hawaiian Islands. The aircraft performed an emergency landing in Kahului Airport, Maui.
- In 2002, a 45 year old C130A Firefighting Tanker Aircraft had its wings fail in flight. Metallurgical investigation of the wreckage showed *extensive fatigue damage to the wings*

The basic elements of modern-day fatigue and damage-tolerance based methodology were forged from the lessons learned from these and other accidents that occurred in the last half-century of aircraft operations.

1. **Design of Pressurized Fuselages:** The *Comet* accident taught us that a pressurized fuselage must be equipped with sufficient *crack-arrest features* in order to contain any cracking that may occur.
2. **Fatigue Life Assurance Philosophy:** The *F-111* accident taught us not to completely rely on *safe-life* methodology, since it is not sufficiently robust to deal with initial flaws. The *Lusaka* accident demonstrated the fallacy of the *fail-safe* principle, when *not* combined with adequately defined structural inspections. The present-day damage-tolerance concept was born as a result of these incidents. The *Aloha* accident taught us the dangers of *aging fleets, multiple-site-damage, widespread-fatigue-damage* and other concepts that were not considered in the fatigue regulations of that era.
3. **Fatigue Testing:** The *Comet* accident taught us that a fatigue test should *not* be performed on a test-article that has previously seen unrepresentative loading. The *Lusaka* accident demonstrated the need to perform full-scale fatigue testing of newly designed structures.
4. **Fatigue Loading Spectra:** the *Lusaka* accident showed the need to perform flight test measurements in order to confirm the adequacy of the loading spectrum used for analysis and testing. The *C130A* ongoing problem shows the importance of matching the loading spectrum to the actual mission, especially when drastic changes to the mission-profiles occur.

11.6 REFERENCES

1. Brot, A., "Review of Aeronautical Fatigue Investigations in Israel, April 2003 – March 2005", *Minutes of the 29th ICAF Conference*, Hamburg, Germany, 2005.
2. Brot, A. and Matias, C., "An Evaluation of the Strip-Yield Retardation Model for Crack Growth Prediction under Spectrum Loading", *Proceeding of the 24th ICAF Symposium*, 2007.
3. Perl, M. and Perry, J. "An Experimental-Numerical Determination of the Three Dimensional Autofrettage Residual Stress Field Incorporating Bauschinger Effects", *J. of Pressure Vessel Technology*, Vol. 128, p. 173, 2006.
4. Perl, M., Levy, C. and Rallabhandy, V., "The Bauschinger Effect's Impact on the 3-D Combined SIFs for Radially Cracked Fully or Partially Autofrettaged Thick-Walled Cylinders", *CMES*, Vol. 11, no. 1, 2006.
5. Perry, J., Perl, M., Shneck, R. and Haroush, S., "The Influence of the Bauschinger Effect on the Yield Stress, Young's Modulus and Poisson's Ratio of a Gun Barrel Steel", *J. of Pressure Vessel Technology*, Vol. 128, p. 179, 2006.
6. Perl, M., Levy C. and Rallabhandy, V., "The Influence of the Bauschinger Effect on 3D Stress Intensity Factors for Internal Radial Cracks in a Fully or Partially Autofrettaged Gun Barrel", *J. of Pressure Vessel Technology*, Vol. 128, p. 233, 2006.
7. Brot, A., and Matias, C., "Residual Tensile Stresses Induced by Cold-Working a Nearby Fastener Hole", *Proceedings of the 47th Israel Annual Conference on Aerospace Sciences*, 2007.

8. Granot, Z., "Simplified Methods for Predicting Fatigue Life of Composite Material Structures", *Proceedings of the 23rd ICAF Symposium*, 2005.
9. Kressel, I et al., "Damage Tolerance of Bonded Composite Repairs – Analysis and Tests", *Proceedings of the 23rd ICAF Symposium*, 2005.
10. Kressel, I et al., "Smart Bonded Composite Patch Repairs – Analysis and Testing", *Proceeding of the 24th ICAF Symposium*, 2007.
11. Pevzner, P., Berkovits, A., et al, "A Novel Approach for Damage Detection in Composites", *Proceedings of the 47th Israel Annual Conference on Aerospace Sciences*, 2007.
12. Botesev, M., Kressel, I., et al, "Structural Health Monitoring for Composite Structures Based on Lamb Waves Detection by Embedded Fiber Bragg Gratings", *Proceedings of the 47th Israel Annual Conference on Aerospace Sciences*, 2007.
13. Matias, C., Brot, A. and Senderovits, W., "Defining Experimentally the Probability of Detection of Hidden Second-Layer Cracks", *Proceedings of the USAF Aircraft Structural Integrity Program Conference*, 2006.
14. Omer N., Yosibash Z, "On the Path Independency of the Pointwise J-Integral in 3-D Domains", *International Journal of Fracture*, vol. 136, pp. 1-36, 2005.
15. Yosibash Z., Omer N., Costabel M. and Dauge, M., "Edge Stress Intensity Functions in Polyhedral Domains and their Extraction by a Quasidual Function Method", *International Journal of Fracture*, vol. 136, pp. 37-73, 2005.
16. Yosibash Z. and Omer N., "Numerical Methods for Extracting Edge Stress Intensity Functions in Anisotropic Three Dimensional Domains", *Computer Methods in Applied Mechanics and Engineering*, to appear in 2007.
17. Yosibash Z., Priel E. and Leguillon, D., "A Failure Criterion for Brittle Elastic Materials under Mixed-Mode Loading", *International Journal of Fracture*, vol. 141, no. 1, pp. 291-312, 2006.
18. Priel E., Bussiba A., Gilad I. and Yosibash Z., "Mixed Mode Failure Criteria for Brittle Elastic V-Notched Structures", *International Journal of Fracture*, Submitted for publication.
19. Banks-Sills, L., Wawrzynek, P.A., Carter, B., Ingraffea, A.R. and Hershkovitz, I., "Methods for Calculating Stress Intensity Factors in Anisotropic Materials: part II – Arbitrary Geometry", *to appear in Engineering Fracture Mechanics*.
20. Banks-Sills, L., Hershkovitz, I., Wawrzynek, P.A., Eliasi, R. and Ingraffea, A.R., "Methods for Calculating Stress Intensity Factors in Anisotropic Materials: part I – $z = 0$ is a Symmetric Plane". *Engineering Fracture Mechanics* vol. 72, pp.2328–235, 2005.
21. Dorogoy, A. and L. Banks-Sills, L., "Effect of Crack Face Contact and Friction on Brazilian Disk Specimens - a Finite Difference Solution", *Engineering Fracture Mechanics* vol. 72, pp. 2758–2773, 2005.
22. Dorogoy, A. and Banks-Sills, L., "Shear Loaded Interface Crack under the Influence of Friction - a Finite Difference Solution", *International Journal for Numerical Methods in Engineering* vol. 59, pp. 1749–1780, 2004.
23. Banks-Sills, L., Freed, Y., Eliasi, R. and Fourman, V., "Fracture Toughness of the +45°/-45° Interface of a Laminate Composite", *International Journal of Fracture* vol. 141, pp.195–210, 2006.
24. Banks-Sills, L., Boniface, V. and Eliasi, R., "Development of a Methodology for Determination of Interface Fracture Toughness of Laminate Composites – the 0°/90° pair", *International Journal of Solids and Structures* vol. 42, pp. 663–680, 2005.

25. Rabinovich, D., Givoli, D. and Vigdergauz, S, "Crack Detection Without Remeshing Using a Genetic Algorithm", *Proceedings of the 47th Israel Annual Conference on Aerospace Sciences*, 2007.
26. Rabinovich, D., Givoli, D and Vigdergauz, S., "XFEM Crack Detection Scheme Using a Genetic Algorithm", *to appear in the International Journal for Numerical Methods in Engineering*.
27. Karp, B., Rittel, D. and Durban, D., "Health Monitoring of Structural Joints", *Proceedings of the 47th Israel Annual Conference on Aerospace Sciences*, 2007.
28. Ben-Noon, M., Grosu, E. and Jiny, S., "Fleet Usage Spectrum Evaluation and Mission Classification", *Proceedings of the USAF Aircraft Structural Integrity Program Conference*, 2006.
29. Brot, A., "Development of Fatigue Life Regulations Based on Lessons Learned from Several Aircraft Accidents", *Proceedings of the 46th Israel Annual Conference on Aerospace Sciences*, 2006.